2018 IEEE-RAS 18th International Conference on Humanoid Robots (Humanoids)
Beijing, China, November 6-9, 2018

Whole-body Posture Evaluation and Modification for Crane-less Servo-off Operation of Life-sized Humanoid Robot

Masaki Murooka, Yohei Kakiuchi, Kei Okada and Masayuki Inaba

Abstract— **In order to make humanoid robots work in the real world, it is necessary to construct a robot system that can be operated without any crane support from start to finish. This paper deals with crane-less servo-off operation of life-sized humanoid robot in which a robot safely turns off / on the joint servo without relying on external physical support. We organize the necessity and difficulty of life-sized humanoid servo-off and introduce a post-evaluation based heuristic procedure of generating servo-off posture. By generated servo-off posture and scripted transition motion, we demonstrate the crane-less servo-off operation with real life-sized humanoid robots in several scenarios.**

I. Introduction

A life-sized humanoid is expected to continuously work in various situations, such as disaster response and daily life assistance, taking advantage of the same body structure as a human being. In order to operate a life-sized humanoid in the real world, it is not enough to develop elemental functions for realizing tasks such as motion planning and balance control. Only when a comprehensive robot system including operational functions such as coping with low battery level and self-diagnosis at the failure occurrence, the robot can start working in the real world. Activation and termination processing is indispensable for a practical system. In the robot system, when it becomes necessary to turn off the power supply or disassemble and repair the robot, it is necessary for the robot in operation to safely transition from the power-on state to the power-off state.

In this paper, we deal with crane-less servo-off operation in which a life-sized humanoid safely turns off the joint servo and then turns on the servo again without relying on support by equipment such as a crane and demonstrate with real robots as shown in Fig. 1. Unlike a manipulator robot and a wheeled robot, since a humanoid robot does not have a base link that can stably receive support force from the environment, we must prepare a kinematically and dynamically feasible posture from a high-dimensional posture space.

Because it is difficult to realize the necessity of such functions in the development on the simulator, and even when using real robots, it is often operated in laboratories where cranes from the ceiling have been serviced, research which targeted the life-sized humanoid servo-off has not been done so far. This paper aims to solve this problem, which is indispensable when future humanoids are put into practical use.

M. Murooka, Y. Kakiuchi, K. Okada and M. Inaba are with Department of Mechano-Infomatics, The University of Tokyo, 7-3-1 Hongo, Bunkyo-ku, Tokyo 113-8656, Japan murooka at jsk.t.u-tokyo.ac.jp

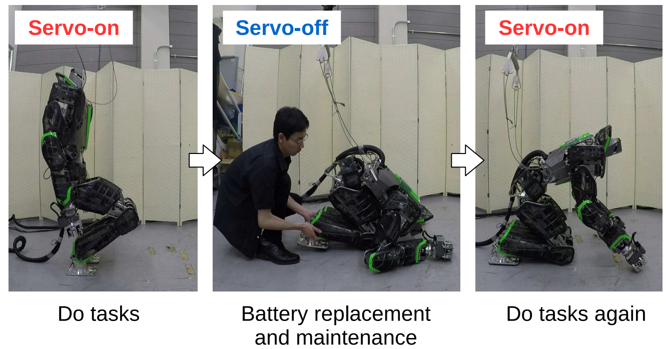

Fig. 1. Scenario of crane-less servo-off operation of life-sized humanoid

A. Related Works

To our knowledge, as there are no papers targeting life-sized humanoid servo-off, we will organize the research on life-sized humanoid in the field related to servo-off and state the position of this research.

1) Real World Task Application of Life-sized Humanoids: In recent years, many research platforms of life-sized humanoid robots have been developed, and various tasks of locomotion and manipulation have been realized by integrating recognition, planning, and control functions [1] [2] [3] [4]. However, many of these demonstrations are realized in a well-maintained laboratory, and the robot is often set in the precise initial position or powered off by being lifted in the air using a safety crane. As a lesson from DARPA Robotics Challenge (DRC) in 2015, the importance of humanoid continuing tasks without external physical support was pointed out [5]. This research aims to make it possible to stop and start a life-sized humanoid robot without a crane equipment.

2) Functions to Cope with Falling: As peripheral functions for practical use which does not directly contribute to the realization of tasks, falling over is studied from both sides of software and hardware. Falling is an important subject for humanoids even after a humanoid that can fall over safely and stand up again is developed [6]. Passive posture control [7], servo gain control during falling [8], impact mitigation by airbag [9], and mechanical robustness by hard points [10] are studied. The crane-less servo-off that this paper tackles is also positioned as the peripheral function of the robot system, which is indispensable for all life-sized humanoids.

B. Contributions and Overview of This Paper

The contributions of this paper are as follows: (i) organizing the crane-less servo-off operation, (ii) evaluation

978-1-5386-7282-2/18/$31.00 ©2018 IEEE

and modification of whole-body posture for servo-off, (iii) realization of crane-less servo off / on by life-sized humanoid robot.

In the following, Sec. II organizes the servo-off of the robot. Sec. III describes the heuristic procedure of posture generation for servo-off. In Sec. IV, servo-off experiments with real life-sized humanoid robots are shown.

II. Discussion on Robot Servo-off

A. Necessity of Crane-less Servo-off Operation

Even a robot with high availability can require servo-off. For the purpose of turning off the servo of robot, the following can be considered:

1) Rest in a safe state when not in operation.
2) Disconnect power supply to replace the battery.
3) Perform maintenance work such as inspection and parts replacement.

For 3), the following must be satisfied:

3-a) Posture does not collapse even if a human moves each limb of the robot's whole-body.
3-b) Human hands can access all parts of the robot's whole-body.

The conditions of 3-a) and 3-b) cannot be realized in one servo-off posture. Therefore, a plurality of servo-off posture candidates should be prepared and used properly so as to realize the above conditions.

B. Examples and Classification of Robot Servo-off

Fig. 2 shows the servo-off state of various types of robots.

1) Servo-off of Mobile Manipulator: In a mobile manipulator robot with wheeled base, since the base has a sufficiently large mass and wide support area, it is not necessary to consider falling at the time of servo-off. Unless the potential energy is too large, the manipulator arm falls gently with servo-off. By back driving, all parts of the robot can be accessed by human hand. However, only when accessing the bottom of the base, jacking up is necessary. Fig. 2 (A) shows an example of mobile manipulator servo-off.

2) Servo-off of Small Humanoid: Many small humanoids that can be lifted by hands can turn off the servo with a squatting posture by bending the knees from an upright posture. This posture, whose stability is not good, is easy to fall over by disturbance. However, it is used because the damage is small due to small mass even if the robot falls over. Fig. 2 (B) shows an example of small humanoid servo-off.

3) Servo-off of Life-sized Humanoid: For life-sized humanoids, stable servo-off without whole-body contact with environment is impossible because the ratio of the torque generated by its own weight to the joint friction torque is large. Therefore, a life-sized humanoid is often servo-off with being supported by the crane and receiving no reaction force from the floor. This type of servo-off guarantees safety and ease of access to all parts of the robot's body, but because it requires a crane equipment, it is inappropriate when the robot is operated on site. As exceptions, pepper in Fig. 2 (C), which has wheeled base, and DRC-HUBO [3], which can transition to wheel support mode, can turn off servo without crane.

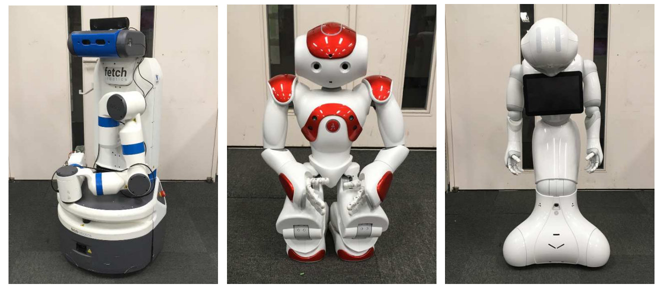

(A) Fetch[1] (B) NAO[2] (C) Pepper[3]

Fig. 2. Servo-off state of various types of robots

C. Difficulty of Crane-less Servo-off of Life-sized Humanoid

The difficulties of crane-less servo-off operation for life-sized humanoids include the following: (i) Motion generation is difficult due to the multilink system which does not have a dynamically stable base link. (ii) Dynamic feasibility cannot be determined intuitively due to multi-contact with self-link and environment. (iii) Large impact occurs when the posture is collapsed by servo-off because of large mass. As the first step towards such difficulties, this paper aims to show example operations realized by real robots even by using ad-hoc method.

III. Servo-off Posture Generation

A. Procedure of Post-evaluation based Posture Generation

In this section, we deal with the problem of generating the target posture of final servo-off state. In general, humanoids can turn off the servo by a supine or prone posture. However, it is desirable to be able to turn off the servo with a more compact posture, as a life-sized humanoid needs large space for lying down.

The posture of a humanoid with two arms and two legs can be generated based on the human posture [11]. When robot servo is turned off, since multiple contacts with self-link and environment occur, which is sensitive to the modeling difficult factors such as friction and deflection, searching servo-off posture automatically from scratch is an inefficient approach. In this paper, we use heuristic generation procedure, in which whole-body posture is first made manually with reference to the rough type of human posture [12] [13] and then evaluated and modified with the method described below. In the manual posture generation, we used the whole-body inverse kinematics that can specify the pose of an arbitrary point on the body and direct designation of the

[1]https://fetchrobotics.com/

[2]https://www.softbankrobotics.com/emea/en/robots/nao

[3]https://www.softbankrobotics.com/emea/en/robots/pepper

joint angle in the interpreter environment of programming language EusLisp[4] with 3D robot model viewer.

The conditions that the servo-off posture of the humanoid should satisfy are listed below:

1) There is no self-collision or environment collision.
2) The joint angle falls within the range of motion.
3) The balance of the whole-body is satisfied.
4) The joint does not move due to friction torque.

1) and 2) are geometric conditions, and 3) and 4) are static conditions. Although it is easy to generate a rough posture in the manual posture generation, it is difficult to guarantee that these constraints are strictly satisfied. Therefore, we introduce a method of evaluating whether posture satisfies the conditions 3, 4 and a method of modifying posture partially so that the posture satisfies the conditions 1, 2, 4. Hereafter, letting n be the number of joints of the robot, a vector obtained by combining the base link position / orientation and the joint angle is referred to as posture $\boldsymbol{\theta} \in \mathbb{R}^{n+6}$.

B. EoM based Posture Feasibility Evaluation

1) Feasibility Evaluation: The static / dynamic conditions of servo-off posture can be expressed as equations of motion (EoM) of multi-link system with inequality constraint. Based on constrained inverse dynamics formulation [14], whether EoM have a solution or not is expressed by the following formula:

$$^{\exists}\boldsymbol{u},\ \boldsymbol{w}_{all} \tag{1}$$

$$\text{s.t.} \quad \begin{pmatrix} \boldsymbol{w_g} \\ \boldsymbol{\tau_g} \end{pmatrix} = \begin{pmatrix} \boldsymbol{0} \\ \boldsymbol{u} \end{pmatrix} + \sum_{c \in \mathcal{C}_{ex}} \begin{pmatrix} \boldsymbol{G}_c^{ex} \\ \boldsymbol{J}_c^{ex\,T} \end{pmatrix} \boldsymbol{w}_c^{ex} + \sum_{c \in \mathcal{C}_{in}} \left\{ \begin{pmatrix} \boldsymbol{O} \\ \boldsymbol{J}_{c^+}^{in\,T} \end{pmatrix} \boldsymbol{w}_{c^+}^{in} + \begin{pmatrix} \boldsymbol{O} \\ \boldsymbol{J}_{c^-}^{in\,T} \end{pmatrix} \boldsymbol{w}_{c^-}^{in} \right\} \tag{2}$$

$$\boldsymbol{w}_{c^+}^{in} + \boldsymbol{w}_{c^-}^{in} = \boldsymbol{0} \quad (c \in \mathcal{C}_{in}) \tag{3}$$

$$\boldsymbol{A}_c \boldsymbol{w}_c \geq \boldsymbol{b}_c \quad (c \in \mathcal{C}_{ex} \cup \mathcal{C}_{in}) \tag{4}$$

$$-\boldsymbol{u}_{fric} \leq \boldsymbol{u} \leq \boldsymbol{u}_{fric} \tag{5}$$

$$\text{where} \quad \boldsymbol{w_g} = \begin{pmatrix} m\boldsymbol{g} \\ \boldsymbol{p_g} \times m\boldsymbol{g} \end{pmatrix} \tag{6}$$

$$\boldsymbol{\tau_g} = ID(\boldsymbol{0}, \boldsymbol{0}, \boldsymbol{\theta}) \tag{7}$$

Eq. (2) is the EoM of the multi-link system, eq. (3) is the constraint of the self-contact wrench, and eq. (4), eq. (5) are the inequality constraint. $\mathcal{C}_{ex}$ and $\mathcal{C}_{in}$ represent a set of all environment contacts and self-contacts, respectively. $\boldsymbol{w}_c^{ex}$ is an external wrench (force / moment) that the robot receives from environment contact, and $\boldsymbol{w}_{c^+}^{in}, \boldsymbol{w}_{c^-}^{in}$ is an action-reaction pair of the self-contact wrench that the robot receives from self-contact as shown in Fig. 3. $\boldsymbol{w}_{all}$ is a vector in which $\boldsymbol{w}_c^{ex} (c \in \mathcal{C}_{ex})$ and $\boldsymbol{w}_{c^+}^{in}, \boldsymbol{w}_{c^-}^{in} (c \in \mathcal{C}_{in})$ are arranged. $\boldsymbol{u}$ represents the torque exerted by the joint, and $\boldsymbol{u}_{fric}$ represents the maximum torque that can passively be exerted when the servo is off due to the friction of the joint [5].

[4]https://github.com/euslisp/EusLisp

[5]This friction torque is referred to as overdrive starting torque in harmonic drive. Reference manual of harmonic drive: https://www.hds.co.jp/products/data/pdf/technicaldocument/hd/CSF-3_Series_Manual_en_0710-2R-TCSF3-E.pdf

$\boldsymbol{G}_c^{ex/in}$ and $\boldsymbol{J}_c^{ex/in}$ are the grasp matrix and Jacobian of the contact point c, respectively, and letting $\boldsymbol{p}_c$, $\boldsymbol{v}_c$, $\boldsymbol{\omega}_c$ be the position, velocity, and angular velocity of the contact point c, the following relationships hold:

$$\boldsymbol{G}_c^{ex/in} = \begin{pmatrix} \boldsymbol{E_3} & \boldsymbol{O_3} \\ [\boldsymbol{p}_c \times] & \boldsymbol{E_3} \end{pmatrix} \tag{8}$$

$$\begin{pmatrix} \boldsymbol{v}_c \\ \boldsymbol{\omega}_c \end{pmatrix} = \boldsymbol{J}_c^{ex/in} \dot{\boldsymbol{\theta}} \tag{9}$$

$\boldsymbol{A}_c$ and $\boldsymbol{b}_c$ represent linearized constraints that contact wrench $\boldsymbol{w}_c$ should satisfy, such as constraints of unilateral force, friction, and center of pressure [14]. $ID(\ddot{\boldsymbol{\theta}}, \dot{\boldsymbol{\theta}}, \boldsymbol{\theta})$ is a function that returns the joint torque by inverse dynamics calculation. Letting m and $\boldsymbol{p_g}$ be the total mass and center of gravity of the robot, $\boldsymbol{w_g}$ and $\boldsymbol{\tau_g}$ represent the wrench and joint torque by own weight, respectively.

Eq. (1) is a linear feasibility problem, which is solvable with an optimization solver. From eq. (1), we can determine feasibility of posture $\boldsymbol{\theta}$ with the following flow:

$$\boldsymbol{\theta} \xrightarrow{ID} (\boldsymbol{w_g}, \boldsymbol{\tau_g}) \xrightarrow{eq.\ (1)} (\boldsymbol{u}, \boldsymbol{w}_{all}) \rightarrow \textit{feasibility} \tag{10}$$

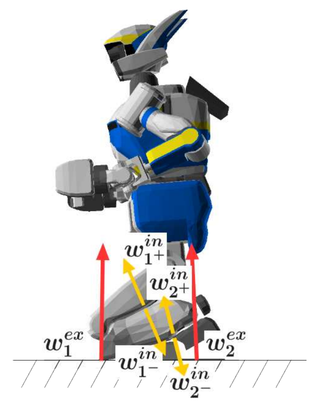

Fig. 3. Wrenches in self-contacts and environment contacts

2) Torque Error Evaluation: For manually correcting the posture, it is useful to evaluate which part should be modified when the posture is infeasible without satisfying the static conditions. By adding torque error to eq. (1) and calculating the minimum error by optimization, it is possible to investigate at which joint of the whole-body the joint torque condition for servo-off is broken.

Letting $\boldsymbol{\varepsilon}$ be the joint torque error, the minimum-norm error is derived by the following formula:

$$\min_{\boldsymbol{u}, \boldsymbol{w}_{all}, \boldsymbol{\varepsilon}} \boldsymbol{\varepsilon}^T \boldsymbol{\varepsilon} \tag{11}$$

$$\text{s.t.} \quad eq.\ (2), eq.\ (3), eq.\ (4)$$

$$-\boldsymbol{u}_{fric} \leq \boldsymbol{u} + \boldsymbol{\varepsilon} \leq \boldsymbol{u}_{fric} \tag{12}$$

Letting $\boldsymbol{x} = (\boldsymbol{u}^T\ \boldsymbol{w}_{all}^T\ \boldsymbol{\varepsilon}^T)^T$, eq. (11) is expressed in the form of quadratic programming (QP) as follows:

$$\min_{\boldsymbol{x}} \quad \boldsymbol{x}^T \begin{pmatrix} \boldsymbol{O} & \boldsymbol{O} & \boldsymbol{O} \\ \boldsymbol{O} & \boldsymbol{O} & \boldsymbol{O} \\ \boldsymbol{O} & \boldsymbol{O} & \boldsymbol{E} \end{pmatrix} \boldsymbol{x} \tag{13}$$

$$\text{s.t.} \quad \begin{pmatrix} \boldsymbol{O} & \boldsymbol{G}_{all} & \boldsymbol{O} \\ \boldsymbol{E} & \boldsymbol{J}_{all} & \boldsymbol{O} \\ \boldsymbol{O} & \boldsymbol{G}_{in} & \boldsymbol{O} \end{pmatrix} \boldsymbol{x} = \begin{pmatrix} \boldsymbol{w_g} \\ \boldsymbol{\tau_g} \\ \boldsymbol{0} \end{pmatrix} \tag{14}$$

$$\begin{pmatrix} \boldsymbol{E} & \boldsymbol{O} & \boldsymbol{E} \\ -\boldsymbol{E} & \boldsymbol{O} & -\boldsymbol{E} \\ \boldsymbol{O} & \boldsymbol{A}_{all} & \boldsymbol{O} \end{pmatrix} \boldsymbol{x} \geq \begin{pmatrix} -\boldsymbol{u}_{fric} \\ -\boldsymbol{u}_{fric} \\ \boldsymbol{b}_{all} \end{pmatrix} \tag{15}$$

$\boldsymbol{G}_{all}$ and $\boldsymbol{J}_{all}$ are matrices in which $\boldsymbol{G}_c^{ex/in}$ and $\boldsymbol{J}_c^{ex/in}$ are arranged side by side, respectively. $\boldsymbol{G}_{in}$ is a matrix representing eq. (3).

The evaluation results of servo-off postures are shown in Fig. 4. In various types of postures based on the basic human postures, it is evaluated whether humanoids can servo off, or which joints have problem when it cannot be done by solving QP of eq. (13).

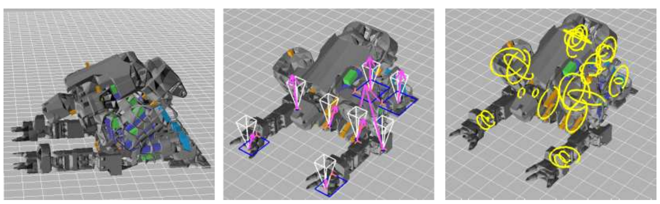

(A) posture to bend elbows and knees (servo-off feasible)

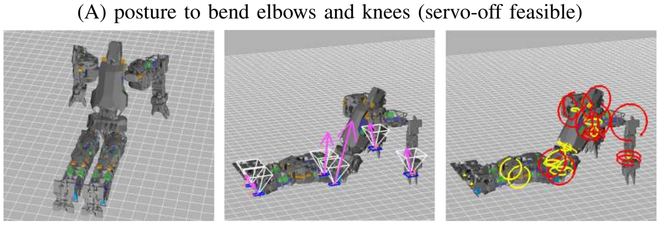

(B) posture to stretch legs and put hands behind (servo-off infeasible)

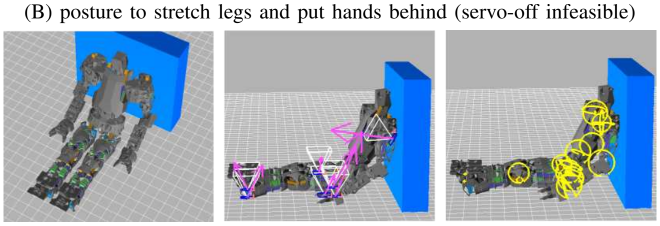

(C) posture to stretch legs and lean against wall (servo-off feasible)

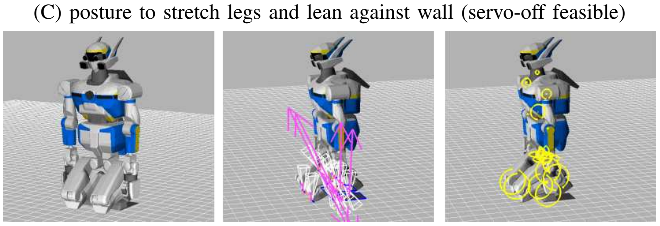

(D) knee standing posture (servo-off feasible)

Fig. 4. Results of EoM based posture evaluation
The evaluation results of four types of servo-off postures are shown. The middle column figures show the contact wrench, and the right column figures show the joint torque, that is necessary in servo-off state. Joint torque that does not satisfies the maximum friction torque is displayed in red.

3) Limb Free Evaluation: In 3-a) of servo-off purpose in Sec. II-A, we pointed out the necessity that human moves each limb, i.e. arm and leg, of the robot stably by back driving in the servo-off posture for maintenance. This can be determined by EoM based method.

To be able to move a limb stably by back driving, it can be considered that the limb should not receive contact wrench from the environment that contributes to supporting the whole-body. Therefore, if the following linear feasibility problem has a solution, it is determined that the target limb can be moved.

$$^{\exists}\boldsymbol{w}_c^{ex} \ (c \in \tilde{\mathcal{C}}_{ex}) \ \text{ s.t. } \ \tilde{\boldsymbol{w}}_{\boldsymbol{g}} = \sum_{c \in \tilde{\mathcal{C}}_{ex}} \boldsymbol{G}_c^{ex} \boldsymbol{w}_c^{ex}, \quad eq.\ (4) \tag{16}$$

$\tilde{\mathcal{C}}_{ex}$ is a set of contacts excluding the contacts on the target limb from $\mathcal{C}_{ex}$, and $\tilde{\boldsymbol{w}}_{\boldsymbol{g}}$ is a wrench by own weight when excluding the target limb.

C. Dynamics Simulation based Posture Modification

When the servo is turned off, the robot moves so that the potential energy of each link decreases due to gravity, and reaches a steady posture accompanied by contacts at whole-body region. In the IK based method requiring the goal position / orientation of Cartesian coordinate, it is difficult to generate a posture that takes into account such contact with the whole-body region. In this paper, we modify the posture in joint angle space using dynamics simulation.

Dynamic simulation of floating base multi-dof system with multiple contacts is difficult to accurately model, and the computational cost is high. Therefore, in our method, the posture is partially modified by calculating forward dynamics only for partial joints of the robot. We select the limb (either one of the left and right arms and legs) which the joints with the joint torque error in eq. (13) belong to as modified limb and apply the forward dynamics calculation assuming that the root link of that limb is fixed in the world frame. If the joints of multiple limbs have joint torque error, do this in order for each limb.

Algorithm. 1 shows the posture modification procedure. It is set as the termination condition of the simulation that one of the following occurs: (i) new environment contact occurs, (ii) new self-contact occurs, (iii) reach the boundary of the joint motion range, (iv) become a steady state where the joint velocity is sufficiently small. In the case of (i), add a new environment contact and perform the evaluation of eq. (13) again. In the case of (iv), use the posture at the end of the simulation. In the current implementation, we use forward dynamics calculation to derive natural posture with small potential energy or contact with environment, so limbs that do not satisfy the joint torque condition despite being in contact with the environment are not supported. Therefore, in the case of (ii), (iii) or the case that the result of (i) does not satisfy the joint torque condition, another candidate posture needs to be generated manually again. Fig. 5 shows the examples of case of (ii) self-contact and (iv) steady state. The flow of simulation based posture modification by forward dynamics is represented as follows:

$$\boldsymbol{\theta^{in}} \xrightarrow{FD} \ddot{\boldsymbol{\theta}} \xrightarrow{\int} \boldsymbol{\theta^{modified}}, feasibility \tag{17}$$

Algorithm 1 Simulation based posture modification

Given: $\boldsymbol{\theta}$
$\dot{\boldsymbol{\theta}} \leftarrow \mathbf{0}$
repeat
  $\ddot{\boldsymbol{\theta}} \leftarrow FD(\boldsymbol{\theta}, \dot{\boldsymbol{\theta}}, \boldsymbol{\tau}_{fric})$
  update $\boldsymbol{\theta}, \dot{\boldsymbol{\theta}}$ from $\ddot{\boldsymbol{\theta}}$
until ($\neg$ self/environment-collision) $\wedge$ ($\neg$ joint-limit-over) $\wedge$ ($\neg$ steady-state)
return $\boldsymbol{\theta}$

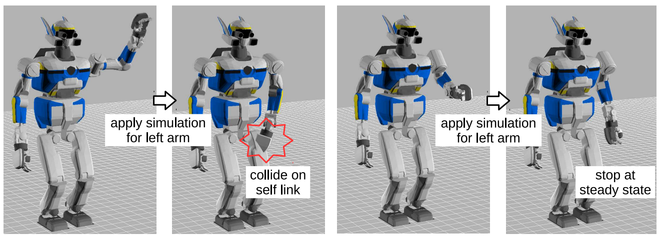

(A) Case that self-collision occurs (B) Case of reaching steady state

Fig. 5. Results of simulation based posture modification

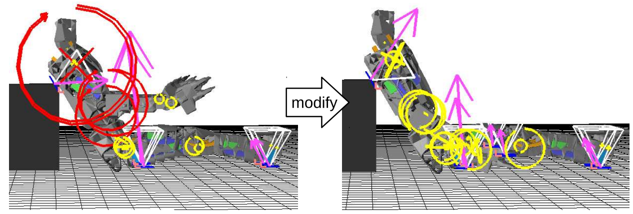

RHP4B servo-off posture for the experiment of Fig. 7 (A)

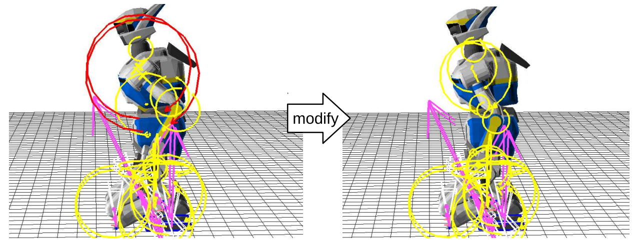

HRP2-JSKNTS servo-off posture for the experiment of Fig. 7 (C)

Fig. 6. Servo-off posture generation in the experiments
Left figures show manually generated postures. The joints which do not satisfy torque condition are shoulder-roll, shoulder-pitch, elbow-pitch, and waist-pitch for RHP4B, and shoulder-pitch for HRP2-JSKNTS. Right figures show postures modified by simulation, which are servo-off feasible.

IV. Servo-off Experiment of Life-sized Humanoid

We performed experiments in which life-sized humanoids transit from standing posture to servo-off posture, turn off the servo, and start moving again by turning on the servo. In these experiments, the rough servo-off posture was first generated manually and then evaluated and modified by the method of Sec. III. The transition posture sequence between the standing posture and the servo-off posture was manually scripted.

Fig. 7 shows the snapshots of the experiments. In (A1)-(A8), RHP4B [10] transitions to a posture to stretch legs and lean against wall and turns off the servo. After confirming that the arms and legs are movable by back driving, the servo is turned on and the robot starts moving again. In (B1)-(B4), RHP4B transitions to a posture to bend elbows and knees and turns off / on the servo. The human can reach hands to the chest and back of the robot in the servo-off postures of (A5), (B3), respectively, so accessibility to the almost whole-body region for maintenance was confirmed. In (C1)-(C4), HRP2-JSKNTS [4] leans against the backrest in the knee standing posture, turns off the servo, and starts moving again after replacing the power battery in the body. In these experiments, crane-less servo-off operation suggested in this paper was realized in multiple scenarios.

Each posture in the experiments was determined that servo-off was feasible by the posture evaluation of Sec. III-B. The posture of Fig. 7 (B3) was manually generated and evaluated as servo-off feasible as shown in Fig. 4 (A). Posture modification by simulation in Sec. III-C was applied to the left and right arms in the postures of Fig. 7 (A5) and (C3). Fig. 6 shows the postures before and after the modification.

Regarding the servo-off in (C3), although it was evaluated that servo-off is feasible even if the robot does not lean on the backrest as shown in Fig. 6, actually the hip-pitch joint moved and the posture collapsed in servo-off state without the backrest. In the torque evaluation of eq. (13), the left and right hip-pitch joints need 2.9 Nm, which is within the range of the friction torque on specifications, in the target servo-off posture, but they need 5.5 Nm and 11.4 Nm if they deviate by 2 degrees and 5 degrees, respectively. Robustness against the joint tracking error and the disturbance caused by work such as battery replacement was raised as a problem.

V. Conclusion

In this paper, we organized the crane-less servo-off operation of life-sized humanoid robot, in which a working robot transits to the safe servo-off posture and turns off / on the joint servo. We described the post-evaluation based heuristic procedure of generating servo-off posture and demonstrated the crane-less servo-off operation with real robots.

In order to improve the completeness of the crane-less servo-off operation, we consider that it should be the next target to control the servo gain for safe servo on / off switching and generate a recovery transition motion automatically from an arbitrary servo-off posture such as after falling.

References

[1] J. Englsberger, A. Werner, C. Ott, B. Henze, M. A. Roa, G. Garofalo, R. Burger, A. Beyer, O. Eiberger, K. Schmid, and A. Albu-Schaffer. Overview of the torque-controlled humanoid robot toro. In *Proceedings of the 2014 IEEE-RAS International Conference on Humanoid Robots*, pp. 916–923, Nov 2014.

[2] F. Negrello, M. Garabini, M. G. Catalano, P. Kryczka, W. Choi, D. G. Caldwell, A. Bicchi, and N. G. Tsagarakis. Walk-man humanoid lower body design optimization for enhanced physical performance. In *Proceedings of The 2016 IEEE International Conference on Robotics and Automation*, pp. 1817–1824, May 2016.

[3] T. Jung, J. Lim, H. Bae, K. K. Lee, H. M. Joe, and J. H. Oh. Development of the Humanoid Disaster Response Platform DRC-HUBO+. *IEEE Transactions on Robotics*, Vol. 34, No. 1, pp. 1–17, Feb 2018.

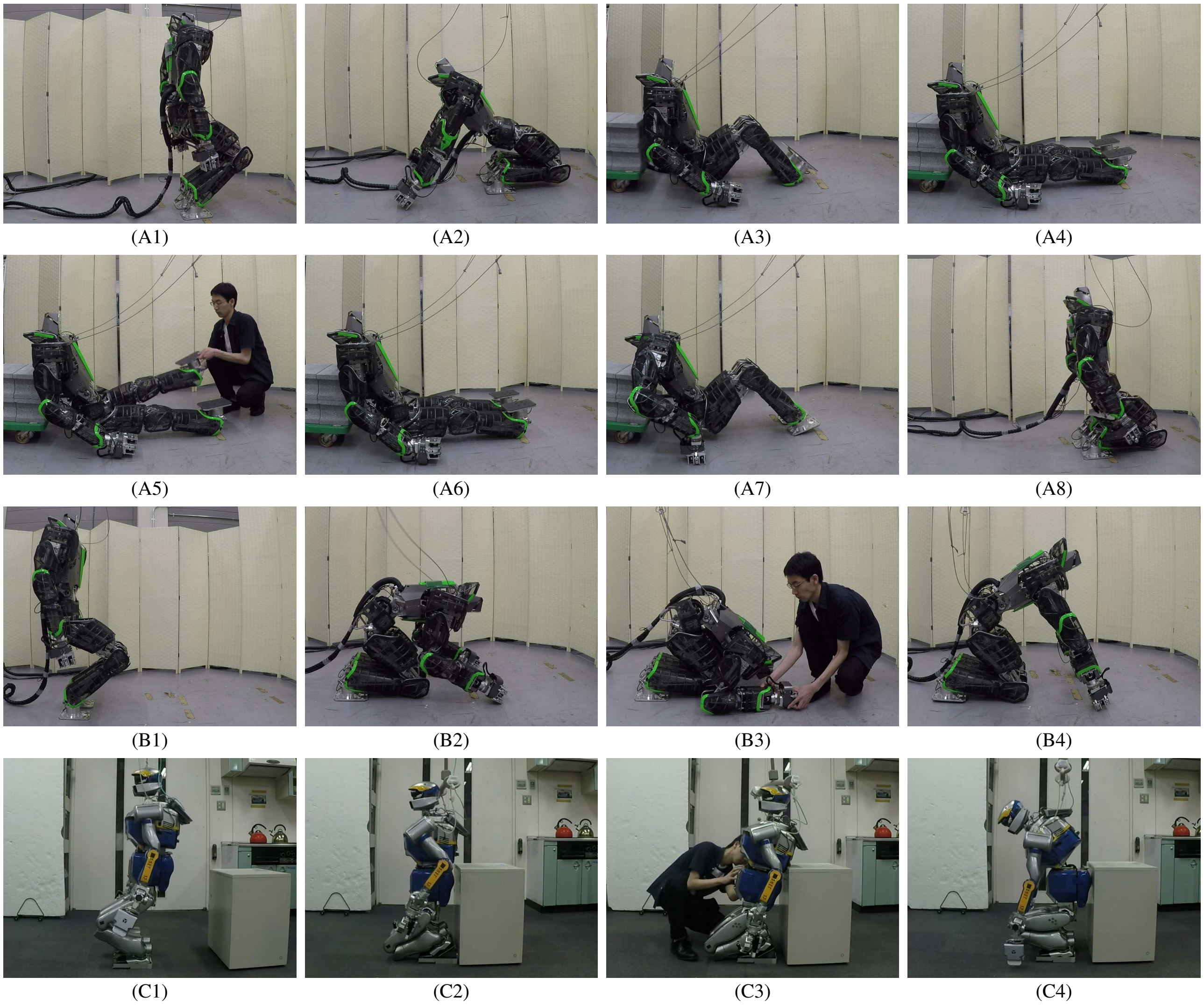

Fig. 7. Snapshots of the servo-off experiment of life-sized humanoid
RHP4B and HRP2-JSKNTS transit from standing posture to servo-off posture, turn off the servo, and start moving again by turning on the servo. The robot servo is turned off in (A5), (B3), and (C3) without crane support.

[4] K. Okada, T. Ogura, A. Haneda, J. Fujimoto, F. Gravot, and M. Inaba. Humanoid motion generation system on HRP2-JSK for daily life environment. In *Proceedings of The 2005 IEEE International Conference on Mechatronics and Automation*, Vol. 4, pp. 1772–1777, July 2005.

[5] C. G. Atkeson, et al. No falls, no resets: Reliable humanoid behavior in the darpa robotics challenge. In *Proceedings of the 2015 IEEE-RAS International Conference on Humanoid Robots*, pp. 623–630, Nov 2015.

[6] K. Fujiwara, F. Kanehiro, S. Kajita, K. Yokoi, H. Saito, K. Harada, K. Kaneko, and H. Hirukawa. The first human-size humanoid that can fall over safely and stand-up again. In *Proceedings of the 2003 IEEE/RSJ International Conference on Intelligent Robots and Systems*, Vol. 2, pp. 1920–1926 vol.2, Oct 2003.

[7] A. Goswami, S. Yun, U. Nagarajan, S. Lee, K. Yin, and S. Kalyanakrishnan. Direction-changing fall control of humanoid robots: theory and experiments. *Autonomous Robots*, Vol. 36, No. 3, pp. 199–223, Mar 2014.

[8] V. Samy, S. Caron, K. Bouyarmane, and A. Kheddar. Post-impact adaptive compliance for humanoid falls using predictive control of a reduced model. In *Proceedings of the 2017 IEEE-RAS International Conference on Humanoid Robots*, pp. 655–660, Nov 2017.

[9] S. Kajita, R. Cisneros, M. Benallegue, T. Sakaguchi, S. Nakaoka, M. Morisawa, K. Kaneko, and F. Kanehiro. Impact acceleration of falling humanoid robot with an airbag. In *Proceedings of the 2016 IEEE-RAS International Conference on Humanoid Robots*, pp. 637–643, Nov 2016.

[10] Y. Kakiuchi, M. Kamon, N. Shimomura, S. Yukizaki, N. Takasugi, S. Nozawa, K. Okada, and M. Inaba. Development of life-sized humanoid robot platform with robustness for falling down, long time working and error occurrence. In *Proceedings of the 2017 IEEE/RSJ International Conference on Intelligent Robots and Systems*, pp. 689–696, Sept 2017.

[11] L. Meng, Z. Yu, X. Chen, W. Zhang, M. Ceccarelli, K. Hashimoto, A. Takanishi, Q. Huang, W. Guo, L. Xie, and H. Liu. A falling motion control of humanoid robots based on biomechanical evaluation of falling down of humans. In *Proceedings of the 2015 IEEE-RAS International Conference on Humanoid Robots*, pp. 441–446, Nov 2015.

[12] J. Kohara, et al. Dynamic bodily measurement for architectural planning. *Transactions of the Architectural Institute of Japan*, Vol. 297, pp. 89–99, 1980.

[13] H. Terakado. Space study on living postures. *The Japanese journal of ergonomics*, Vol. 6, No. 1, pp. 51–56, 1970.

[14] K. Nagasaka, Y. Kawanami, S. Shimizu, T. Kito, T. Tsuboi, A. Miyamoto, T. Fukushima, and H. Shimomura. Whole-body cooperative force control for a two-armed and two-wheeled mobile robot using generalized inverse dynamics and idealized joint units. In *Proceedings of The 2010 IEEE International Conference on Robotics and Automation*, pp. 3377–3383, May 2010.